International Journal of Cardiology 155 (2012) 394–399

Contents lists available at ScienceDirect

International Journal of Cardiology

journal homepage: www.elsevier.com/locate/ijcard

A new automated system to identify a consistent sampling position to make tissue Doppler and transmitral Doppler measurements of E, E′ and E/E′☆,☆☆

Niti M. Dhutia [a,b,*], Graham D. Cole [b], Keith Willson [b], Daniel Rueckert [c], Kim H. Parker [a,b], Alun D. Hughes [b], Darrel P. Francis [b]

[a] Department of Bioengineering, Imperial College of Science, Technology, and Medicine, London SW7 2AZ, United Kingdom
[b] International Centre for Circulatory Health, National Heart and Lung Institute, Imperial College, London, United Kingdom
[c] Department of Computing, Imperial College of Science, Technology, and Medicine, London SW7 2AZ, United Kingdom

ARTICLE INFO

Article history:
Received 12 August 2010
Accepted 23 October 2010
Available online 20 November 2010

Keywords:
Echocardiography
Doppler
Pulsed
Heart failure
Systolic
Heart failure
Diastolic
Automated

ABSTRACT

Background: Transmitral pulse wave (PW) Doppler and annular tissue Doppler velocity measurements provide valuable diagnostic and prognostic information. However, they depend on an echocardiographer manually selecting positions to make the measurements. This is time-consuming and open to variability, especially by less experienced operators. We present a new, automated method to select consistent Doppler velocity sites to measure blood flow and muscle function.
Methods: Our automated algorithm combines speckle tracking and colour flow mapping to locate the septal and lateral mitral valve annuli (to measure peak early diastolic velocity, E′) and the mitral valve inflow (to measure peak inflow velocity, E). We also automate peak velocity measurements from resulting PW Doppler traces. The algorithm-selected locations and time taken to identify them were compared against a panel of echo specialists — the current "gold standard".
Results: The algorithm identified positions to measure Doppler velocities within 3.6 ± 2.2 mm (mitral inflow), 3.2 ± 1.8 mm (septal annulus) and 3.8 ± 1.5 mm (lateral annulus) of the consensus of 3 specialists. This was less than the average 4 mm fidelity with which the specialists could themselves identify the points. The automated algorithm could potentially reduce the time taken to make these measurements by 60 ± 15%.
Conclusions: Our automated algorithm identified sampling positions for measurement of mitral flow, septal and lateral tissue velocities as reliably as specialists. It provides a rapid, easy method for new specialists and potentially non-specialists to make automated measurements of key cardiac physiological indices. This could help support decision-making, without introducing delay and extend availability of echocardiography to more patients.

1. Introduction

Echocardiography, a safe, portable and non-invasive imaging modality is commonly used to make measurements of heart function. An important measurement is the estimation of the peak blood velocity through the mitral valve using pulsed wave (PW) Doppler. The E (the velocity of blood flow across the mitral valve) and E′ (the peak rate at which the ventricle expands to receive this inflow of blood), especially expressed as the E/E′ ratio shows promise as a surrogate of left ventricular filling pressure, with both diagnostic and prognostic value [1,2]. However, selecting the locations to make these measurements, currently needs to be done manually by echo specialists, and in the absence of guidelines stating exactly where to measure, these measurements are open to variability [3,4].

There have been developments in automatic tracing of spectral Doppler traces, using methods such as wave contour detection [5], low-pass filtering, edge detection and thresholding [6,7] and a PHD (probabilistic, hierarchical and discriminant) framework [8,9]. However, these techniques required a human operator to identify the sampling location in order to produce a trace for subsequent automated analysis. Nevo et al. [10] developed a semi-automated system to track mitral valve annulus motion using multidimensional dynamic programming and apodized block matching, however this again required initial manual selection of annulus points.

In this study we use a novel, fully-automated method, which uses speckle tracking and colour flow mapping, to select Doppler measurement positions at the mitral inflow, septal annulus and lateral annulus, and to make measurements of peak E and E′ velocities from the Doppler

☆ The authors are solely responsible for the design and conduct of this study; all study analyses, the drafting and editing of the paper and its final contents. All authors have no conflict of interest to declare.

☆☆ *Grants/Financial suppport:* Darrel Francis was supported by the British Heart Foundation (FS 04/079).

* Corresponding author. ICCH Building, 59-61 North Wharf Road, Paddington, London W2 1LA, UK. Tel.: +44 7716817863.
E-mail address: nmd04@imperial.ac.uk (N.M. Dhutia).

0167-5273/$ – see front matter © 2010 Elsevier Ireland Ltd. All rights reserved.
doi:10.1016/j.ijcard.2010.10.048

traces obtained at these positions, without any human selection of points.

2. Methods

Fig. 1 shows an apical four chamber view, indicating the positions to measure PW Doppler velocities, and typical spectral Doppler traces that would be obtained at each position. Our algorithm which was implemented in MATLAB (Mathworks Inc.) uses a specially devised combination of speckle tracking and colour flow mapping to locate positions to make key Doppler velocity measurements.

2.1. Automated annulus point selection

The first stage was to apply speckle tracking on the greyscale apical four chamber image. Speckles arise from scattering, reflection and interference due to inhomogeneities, and can be used to follow frame-to-frame tissue motion. Our speckle tracking algorithm was implemented using a 2D block matching technique, based on normalized cross correlation.

The motion tracking involves identifying a kernel on one frame of an image, and in the next frame, searching for a matching speckle pattern within a search window surrounding the initial kernel. This process is repeated for equally spaced grids across the whole image, and for all the frames in the video loop. The invalid vectors from the speckle tracking stage were eliminated using image features such as contrast, intensity and neighbourhood consistency of the vectors.

Global image parameters i.e. mean velocity and pixel intensity across time were first used to identify the approximate positions of the septum and two walls in the four chamber view. The vectors were then used to locate three high velocity regions in the image identifying the approximate positions of the septum and free walls. The next step was to locate the exact measurement position of the septal annulus and lateral annulus by finding the point with maximum diastolic velocity within each region. Fig. 2 shows the positions selected automatically by the algorithm.

2.2. Automated mitral inflow point selection

The mitral inflow was located by a combination of speckle tracking and colour flow mapping. The speckle-tracked velocity vectors were first used to extract cardiac timing information by computing the mean of the vertical component of all vectors in each frame. This provided an approximate indication of the start and duration of systole and diastole during the cardiac cycle. Using this information the diastolic frames in the video loop were used to find regions of vectors pointing apically, which distinguished the mitral valve from the rest of the image, since the other cardiac structures move away from the apex in diastole.

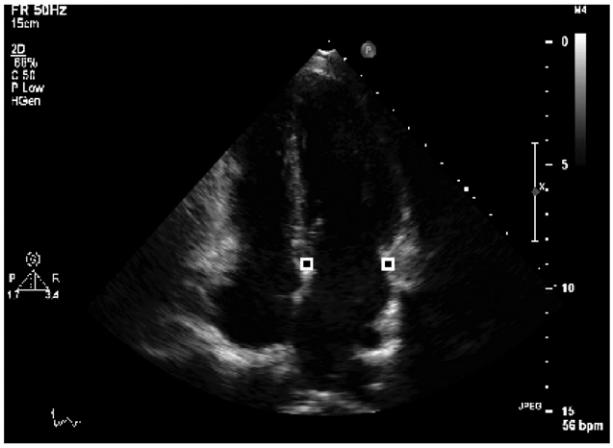

Fig. 2. The square markers at the septal and lateral annuli show the positions selected by the automated algorithm using speckle tracking, without any operator guidance.

The colour flow image of the area identified as the likely mitral valve location was then analysed. The colours in the image were mapped to velocities, and the peak velocity in the analysed area was used as the sampling position for the PW Doppler. Fig. 3 shows an example of the location of the mitral valve inflow identified by the automated algorithm.

2.3. PW Doppler trace peak

After selecting positions to measure PW Doppler velocities, the traces obtained at those positions need to be analysed to find the peak E and E′ velocities. These values are usually obtained by an echo specialist manually placing a cursor on the trace where the value is recorded. Previous studies have been carried out to automate tracing of the velocity envelope, but with the aim of making complex measurements. In this case only the peak velocities are required; therefore a relatively simple approach has been implemented.

The first stage was to apply a thresholding to the image to separate the background from the trace. Background pixels incorrectly detected as foreground pixels could be eliminated by detecting any small unconnected regions, since the peaks in the trace would consist of large connected regions.

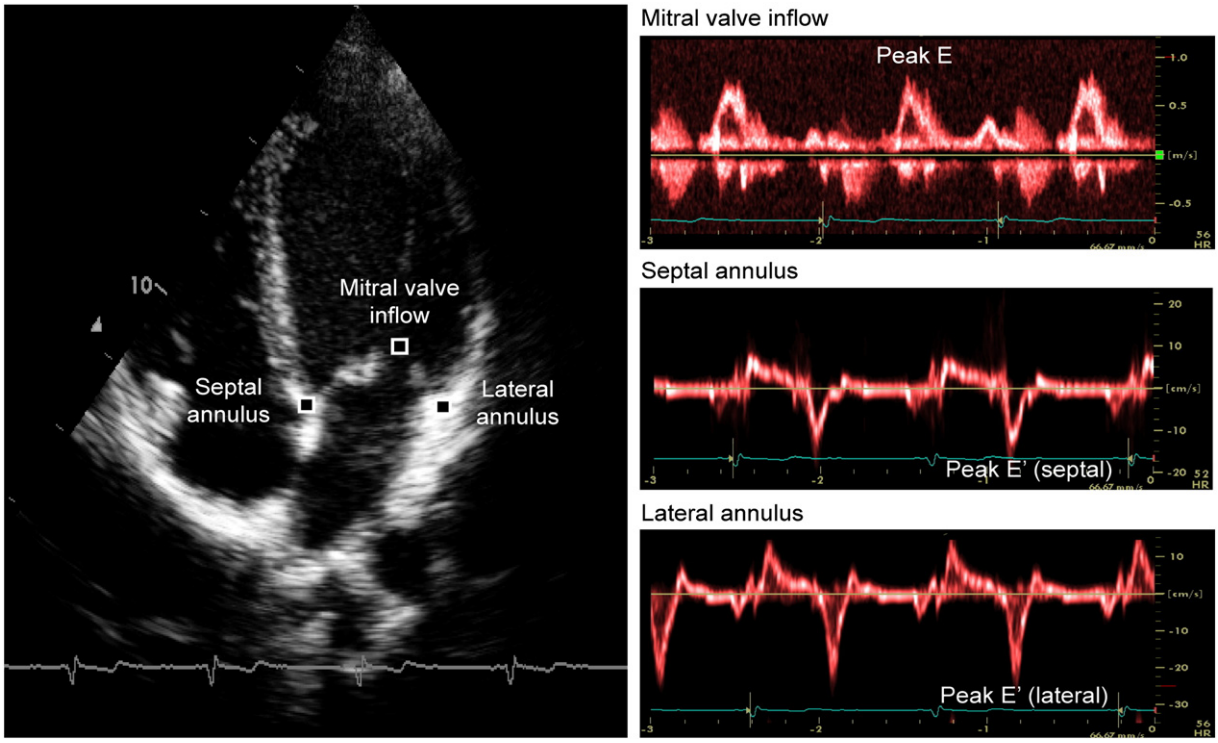

Fig. 1. Left: apical 4-chamber 2D greyscale image obtained from transthoracic echocardiography showing typical positions selected by specialist echo operators to measure PW Doppler at the mitral valve inflow, septal annulus and lateral annulus Right: PW Doppler traces obtained at the 3 positions. Peak of early diastolic waves, E and E′, have been indicated.

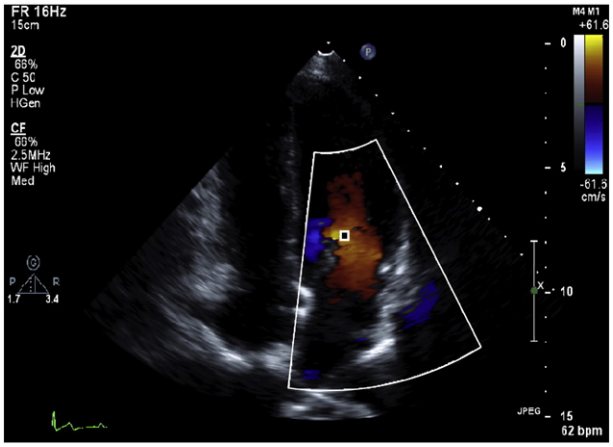

Fig. 3. Apical 4-chamber view freeze frame obtained from colour flow mapping showing blood flow velocity in the left side of the heart. The marker at the at the mitral valve inflow shows the position selected by the automated system using colour flow mapping velocities.

The curve was extracted by selecting a single pixel per column from the thresholded image, based on a biggest gap (group of consecutive black pixels) criterion. For each column the first white pixel at the beginning of the gap was selected. This formed an estimate of the curve envelope, which was smoothed to eliminate noisy regions. The resulting envelope was used to locate the peaks and extract the peak E and E′ values.

2.4. Algorithm validation

2.4.1. Images

The algorithm's performance was validated on 20 echo studies acquired from subjects with no significant echocardiological abnormality using a Phillips IE33 machine. Each study consisted of 2 DICOM video loops of 3 cardiac cycles each; a standard greyscale apical 4 chamber view of the heart and a 4 chamber view with colour flow mapping across the mitral valve. The resolutions of the images were 640×480 or 800×600 pixels, and pixel sizes ranged from 0.33 to 0.63 mm/pixel. The video frame rate was 30 Hz. The images were randomly selected from a database in order to ensure the sample used was representative of a range of image quality to evaluate the performance of the algorithm with a "real world"' cohort. 25 PW Doppler trace images acquired at the mitral inflow, septal annulus and lateral annulus were also used to test the accuracy of automated peak E and E′ measurement.

2.4.2. Data analysis

For each greyscale video, three echo specialists were asked to select three points on the image: the mitral valve inflow in order to measure PW Doppler velocity, the septal annulus of the mitral valve and the lateral annulus to make a tissue Doppler measurement of E′. The time taken by the specialists to make these measurements was compared with the time taken by the algorithm. The videos included the same video repeated in order to assess intra-operator variability. The specialists were also asked to select late diastolic wave peak values from PW Doppler traces.

Due to the lack of a "gold standard" in Doppler velocity measurement positions, the Euclidean average of positions selected by the three specialists was used as a consensus position. In order to evaluate the performance of the automated algorithm in selecting points on the greyscale image, the distances between the algorithm-selected positions and the consensus position was calculated. This was compared to the distances between the positions selected by individual specialists and the consensus position: an inter-operator variability. The intra-operator variability was calculated separately, by re-presentation of images to the same specialists.

The peak values selected by the automated algorithm were compared to the values selected by the specialists, and to the inter-operator and intra-operator variability.

2.5. Statistical analysis

A Bland–Altman analysis [11], was applied to measure agreement between the horizontal (X) and vertical (Y) coordinates of the positions selected by the algorithm and those selected by the specialists, and to measure the agreement between the peak values selected by specialists and the algorithm. The inter-operator variability and errors of the automated method were compared using the 95% confidence intervals for the limits of agreement, and a paired t-test was applied to test the significance of any bias. The time taken by the specialists was also compared to that taken by the algorithm, and a paired t-test was applied to test the significance of any difference. The threshold of statistical significance was taken as $p<0.05$.

3. Results

3.1. Doppler measurement position

Fig. 4 shows freeze frames from 2 video loops, overlaid with the positions selected by individual specialists and the algorithm to

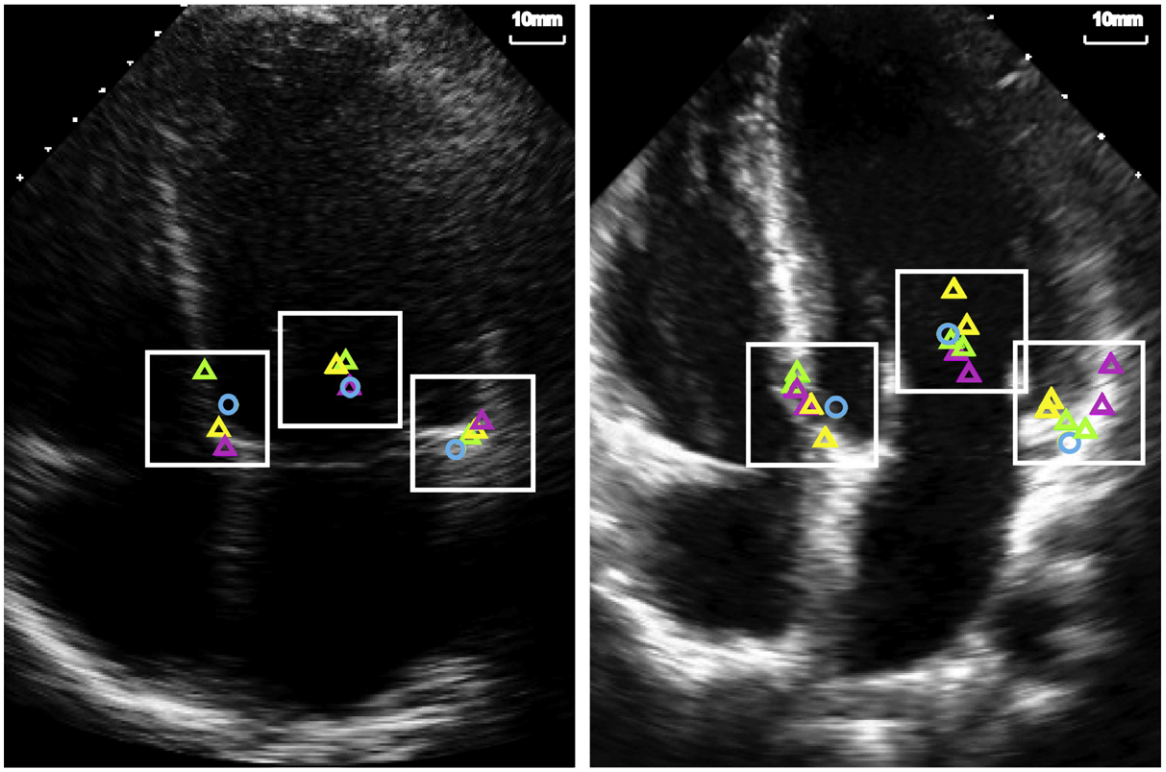

Fig. 4. Apical 4 chamber images showing positions selected by individual specialists (Δ, each colour represents a different specialist) and by the automated algorithm (o) at the mitral valve inflow, septal annulus and lateral annulus.

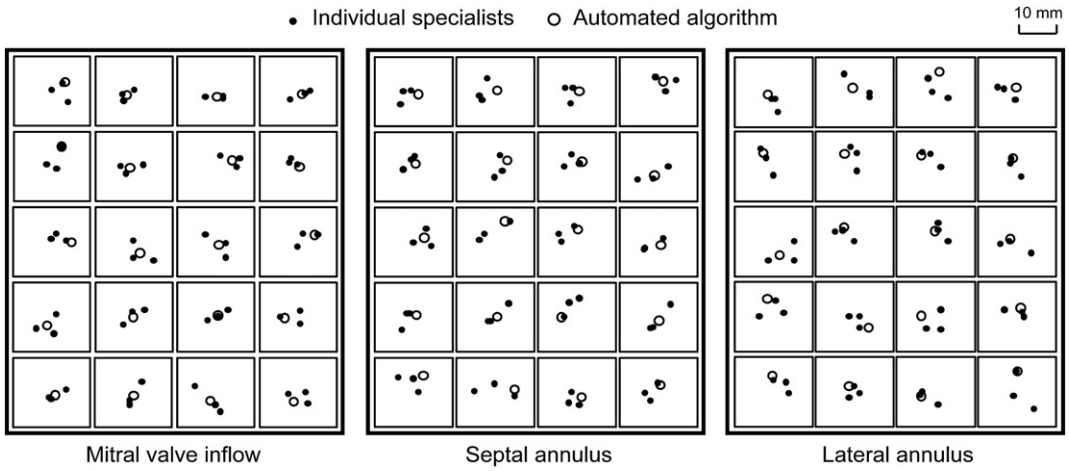

Fig. 5. Plots from 20 different patients (laid out in a 5×4 grid) showing the relative positions selected by specialists (•) and the automated algorithm (o) at the mitral valve inflow, septal annulus and lateral annulus. Each of the smaller boxes represents a small (20×20 mm) region from one patient, as shown in the example in Fig. 4.

measure Doppler velocities. Fig. 5 shows the relative positions selected by specialists and the automated algorithm at each position for all 20 cases. There is significant variability in the positions selected by individual specialists; the algorithm-selected positions lie within the scatter of the specialists.

Fig. 6 shows a comparison of the average distance of positions selected by the algorithm and specialists from the consensus position. The points selected by the automated algorithm were at an average distance of 3.6±2.2 mm (mitral inflow), 3.2±1.8 mm (septal annulus) and 3.8±1.5 mm (lateral annulus) from the consensus position, and specialists selected points at an average distance of 4.5±1.6 mm (mitral inflow), 3.2±1.6 mm (septal annulus) and 3.7±1.5 mm (lateral annulus) from the consensus position. There was no statistically significant difference at the three positions between the algorithm's and individual specialists' closeness to the specialist consensus. The discrepancy between the algorithm and operators was similar to the intra-operator variability; 3.5±2.2 mm (mitral inflow), 3.5±1.8 mm (septal annulus) and 3.9±1.5 mm (lateral annulus), and lower than inter-operator variability; 7.9±1.8 mm (mitral inflow), 5.5±1.9 mm (septal annulus) and 6.3±1.6 mm (lateral annulus).

A Bland–Altman analysis was applied to the X and Y coordinates in each direction. In the X direction, at the septal annulus, the automated algorithm showed a small bias of 1.4 mm towards the left ventricle, and in the Y direction, at the lateral annulus, a small bias of 1.5 mm downward. There was no significant bias in the X direction at the mitral inflow and lateral annulus and in the Y direction at the mitral inflow and septal annulus.

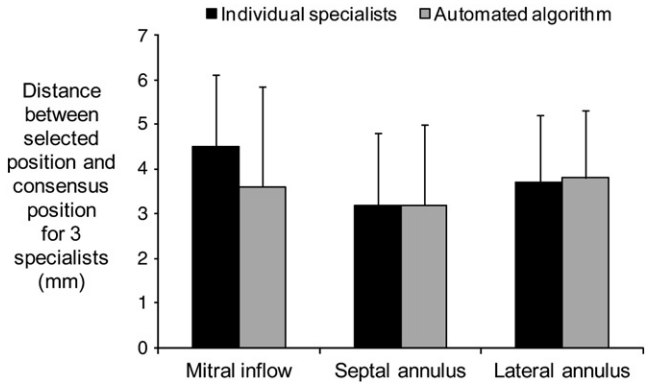

Fig. 6. Comparison between specialists and automated algorithm of the mean distance of selected position from the consensus position for PW Doppler measurements at the mitral inflow, septal annulus and lateral annulus.

The 95% confidence intervals for the limits of agreement of the errors in both methods are shown in Table 1. The inter-operator variability was significantly higher and had wider limits of agreement than the discrepancy between the algorithm and specialists, except in the X direction at the mitral inflow and septal annulus, where there was no statistically significant difference.

3.2. Computation time

The time taken by the specialists and the algorithm to make these measurements is shown in Fig. 7. On average the time required by specialists to make these measurements could be reduced by 60±15% using the automated algorithm. The computation times shown for the algorithm, are projected times based on the assumption that the speckle tracking algorithm used would be real-time.

3.3. PW Doppler trace peak velocity

Fig. 8 shows an example of a PW Doppler trace at the mitral inflow, septal annulus and lateral annulus, with positions to measure peak E wave velocity selected by specialists and the automated algorithm. Bland–Altman analysis showed there was no statistically significant bias in the peak E and E′ measurement. Fig. 9 shows the error in peak value measurements made by specialists and those made by the algorithm. The variability in the measurement of peak value by the algorithm was 2.4±1.4% (mitral inflow), 6.0±4.7% (septal annulus) and 5.0±5.3% (lateral annulus) which was significantly lower than the variability in measurements by specialists; 9.8±5.2% (mitral inflow), 12.1±8.3 (septal annulus) and 8.7±3.1% (lateral annulus). The intra-operator variability at the mitral inflow and septal annulus was relatively low (2.6±3.1% and 3.5±3.3% respectively), and 7.3±4.8% at the lateral annulus.

Table 1
95% confidence intervals for the limits of agreement of the errors in the X and Y direction.

	Automated system (mm)		Inter-operator variability (mm)	
n=20	X	Y	X	Y
Mitral inflow	2.5±0.8*	2.7±0.7	2.6±0.8	6.6±1.6
Septal annulus	2.1±0.6*	1.9±0.8	2.0±0.6	5.3±1.7
Lateral annulus	2.6±0.7	2.5±0.8	3.8±1.1	4.6±1.4

Values expressed as mean±standard deviation. The automated limits of agreement in the X direction at the lateral annulus and all three automated limits of agreement in the Y direction were significantly lower than the inter-operator variability.

* Indicates automated limits of agreement which were not significantly different from the inter-operator variability.

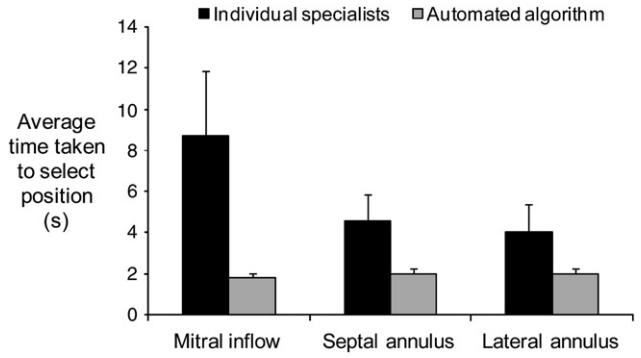

Fig. 7. Comparison between individual the specialists and the automated algorithm of the average time taken to make peak E and E′ measurements.

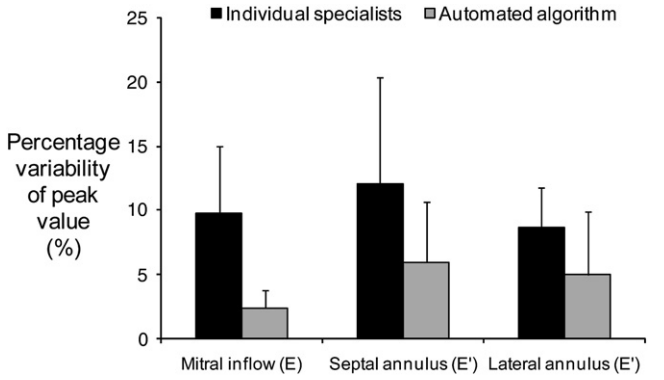

Fig. 9. Comparison between individual specialists and the automated algorithm: Percentage variability in peak E and E′ velocity measurements made from PW Doppler traces.

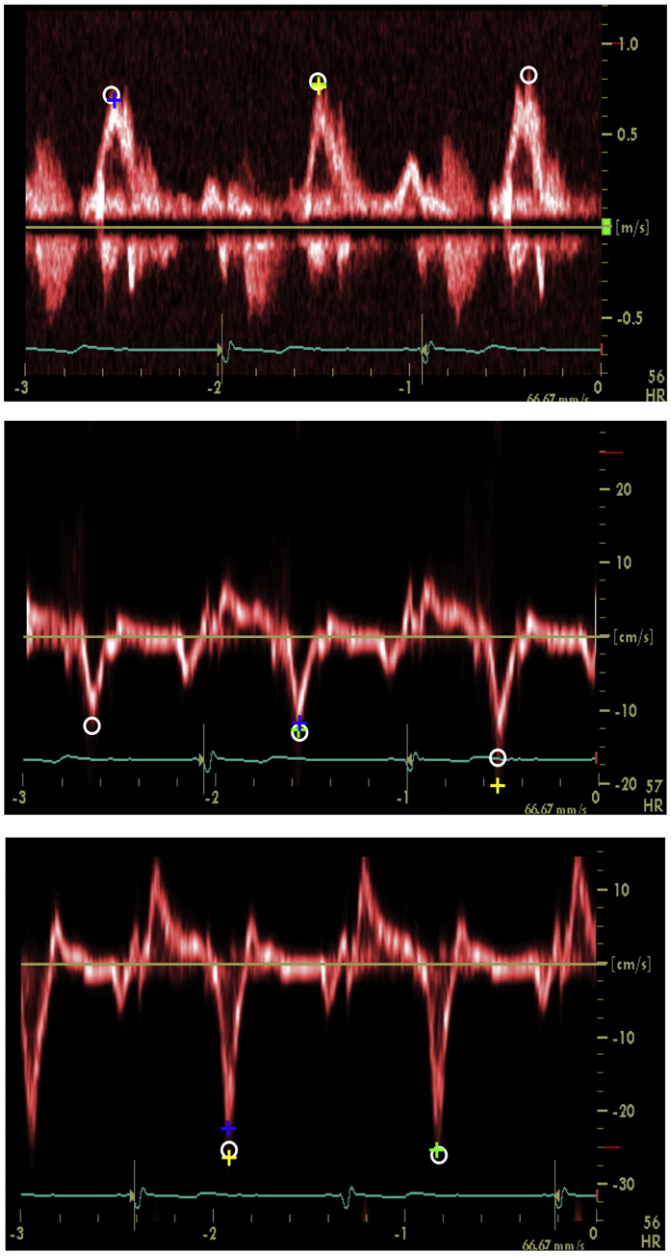

Fig. 8. PW Doppler traces showing peak measurement positions selected by individual specialists (+), each colour represents a different specialist, and the automated algorithm (o) at the mitral valve inflow (top), septal annulus (middle) and lateral annulus (bottom).

4. Discussion

We have developed a novel, fully-automated algorithm to select points to measure mitral valve PW Doppler velocities, and make peak E and E′ velocity measurements from PW Doppler traces. The current necessity for a human operator to select suitable locations for measurement is time-consuming and results in significant operator variability. An automated system would facilitate rapid and reliable measurement of crucial informative echocardiographic parameters, reducing the time required by more than half, would reduce operator variability, and would aid consistency.

Previous studies have focused on automatically tracing PW Doppler traces, but specialists need to manually select points at which these PW Doppler traces are obtained. Our system automates this point selection process, making peak E and E′ velocity measurements without requiring any user interaction. The subjects used had a range of image quality, demonstrating effectiveness with low quality images, such as occurs in patients with poor echo windows.

4.1. How does the automated algorithm compare with human specialists?

Our study shows that a combination of speckle tracking and colour flow mapping can select points to make key PW Doppler velocity measurements as reliably as trained specialists, without needing human intervention. There was significant disagreement between and within specialists in selecting a position: the algorithm consistently selected a position within the cluster of the points selected by different specialists.

4.1.1. Is the bias in positioning important?

Although the Bland–Altman analysis showed a small but statistically significant bias in the X coordinates at the septal annulus and Y coordinates at the lateral annulus, the resulting bias, less than 2 mm, is much smaller than the between-specialist disagreement. The automated system makes these measurements within the fidelity of specialists, and does not increase the degree of error which exists with the current clinical method.

4.2. Potential time saved

The computation time would be significantly reduced using the automated system in comparison to a conventional, purely manual method. This would allow quick measurement of peak velocities, particularly useful in providing consistent data quality in large numbers of subjects undergoing screening.

In the present study, all the automated measurements were made offline. The limiting factor is the length of time taken by the speckle tracking algorithm. Using our proof-of-concept MATLAB system,

speckle tracking takes approximately 5 s per frame, due to the time taken for correlation of each grid with its 256 neighbouring grids. The optimisation of the speckle tracking algorithm is not in the scope of this paper, but, there have been several studies investigating optimisation of speckle tracking for ultrasonic strain imaging [12,13] which show speed can be increased trading off step size and search window size, and using a different grid matching technique, such as the sum of absolute differences. Aside from this, a 10–20 fold speed improvement could be achieved by software and hardware adaptations. The aim of this paper was to focus on the analysis of the vectors after the speckle tracking stage, and future development would only require making the speckle tracking stage real-time, to allow the Doppler measurements to be made during acquisition.

4.3. Peak velocity measurement

Measurement of peak E and E′ velocities showed significant operator variability, and the discrepancy between the algorithm and humans was significantly lower than operator variability for the PW Doppler traces at all three positions. There was no statistically or clinically significant bias observed between the algorithm and the consensus of specialists. The advantage of using the automated algorithm is that it can measure peak velocity over several beats and compute the average without adding to the operator's burden, thus increasing the accuracy of the measurement.

4.4. Study limitations

Due to the lack of definitive standards or independent measurement techniques of peak E and E′ velocity, the performance of our automated algorithm has been tested using the assumption that the average of the measurements made by the echo specialists is a suitable ideal. We believe this is a reasonable assumption because the aim of this system is to make these measurements as reliably as specialists. Of course, since this consensus is derived from the same specialists' judgements, they are statistically advantaged in individually matching this consensus. Therefore, this study shows that the automated algorithm is *at least* as reliable as the specialists.

The images used in this study were taken from an existing database, and were therefore highly compressed with very low frame rates, hindering the speckle tracking element of our algorithm. However, using these compressed images was a good test of ability of the algorithm to provide useful information when presented with poor quality images. If incorporated into an ultrasound system, with access to higher quality images, performance would improve.

Finally, although the data sample used was chosen randomly to have a representative sample it may not be fully representative of all patients: no patients with serious valve or myocardial disease were included. However, since the algorithm does not rely on any specific structures, but rather on velocities within the image, there is no reason why it should not work for a wide range of subjects.

4.5. Clinical implications

This study shows how technology can help automate E, E′ and E/E′ measurements, and hence estimation of left ventricular filling pressure, all of which contribute to the assessment of left ventricular diastolic function.

This may form part of a system which can automatically obtain and calculate E/E′, known to predict invasive measures associated with heart failure, and has prognostic value even in patients with only risk factors for cardiovascular disease [2].

Echocardiography currently exists as a set of tools, packaged in an intimidating, complex piece of hardware. As the cost and size of echocardiographic hardware decreases, the challenge rapidly appearing on the horizon is how to facilitate non-specialists, who will soon have access to this equipment, to make reproducible and valid measurements, on certain limited aspects, to support clinical decisions.

In some patients such as those with heart failure, fluid overload or hypovolemia, serial non-invasive assessments of filling status might be helpful but are not currently conducted because of the disproportionate cost of a full echo scan: in such contexts, the ability of a health care worker with basic training to carry out serial measurements would fulfil a significant current need, for which this approach may be an “enabling technology”.

5. Conclusion

We present a novel, fully-automated method which uses speckle tracking, colour flow mapping and PW Doppler traces, to make measurements of E and E′ and thus calculate E/E′. The system can make these measurements as reliably as experts, with no more difference from the consensus of experts than any individual expert. The system could potentially reduce the time taken to make these measurements by half and could allow physicians, nurses or others without full specialist training in diagnostic echocardiography, to reliably quantify elementary aspects of cardiac performance. This might be developed into a clinically useful tool that would provide a fast, reproducible and non-invasive measurement to assess ventricular dynamics and filling pressure, helping support clinical decision-making without introducing any additional delay and extending the availability of quantitative physiological evaluation to a cohort of patients who would not normally come into contact with an echocardiographer or cardiologist.

Acknowledgements

The authors are grateful to the NIHR Biomedical Research Centre scheme and the BHF Research Excellence Award Centre scheme for providing funding support for this study. The authors of this manuscript have certified that they comply with the Principles of Ethical Publishing in the International Journal of Cardiology [14].

References

[1] Ommen SR, Nishimura RA, Appleton CP, et al. Clinical utility of Doppler echocardiography and tissue Doppler imaging in the estimation of left ventricular filling pressures: A comparative simultaneous Doppler-catheterization study. Circulation 2000;102:1788–94.
[2] Sharp A, Tapp R, Thom S, et al. Tissue Doppler E/E′ ratio is a powerful predictor of primary cardiac events in a hypertensive population: an ASCOT substudy. Eur Heart J 2010;31:747–52.
[3] Khan S, Bess RL, Rosman HS, Nordstrom CK, Cohen GI, Gardin JM. Which echocardiographic Doppler left ventricular diastolic function measurements are most feasible in the clinical echocardiographic laboratory? Am J Cardiol 2004;94:1099–101.
[4] Vinereanu D, Khokhar A, Fraser AG. Reproducibility of pulsed wave tissue Doppler echocardiography. J Am Soc Echocardiogr 1999;12:492–9.
[5] Gaillard E, Kadem L, Pibarot P, Durand LG. Optimization of Doppler velocity echocardiographic measurements using an automatic contour detection method. Engineering in Medicine and Biology Society, 2009. EMBC 2009. Annual International Conference of the IEEE; 2009. p. 2264–7.
[6] Tschirren J, Lauer RM, Sonka M. Automated analysis of Doppler ultrasound velocity flow diagrams. IEEE Trans Med Imaging 2001;20:1422–5.
[7] Greenspan H, Shechner O, Scheinowitz M, Feinberg MS. Doppler echocardiography flow-velocity image analysis for patients with atrial fibrillation. Ultrasound Med Biol 2005;31:1031–40.
[8] Zhou SK. In: Guo F, Park JH, Carneiro G, et al, editors. A probabilistic, hierarchical, and discriminant framework for rapid and accurate detection of deformable anatomic structure; 2007. p. 1–8.
[9] Park J, Zhou SK, Jackson J, Comaniciu D. Automatic mitral valve inflow measurements from Doppler echocardiography. Med Image Comput Comput Assist Interv 2008;11:983–90.
[10] Nevo ST, van Stralen M, Vossepoel AM, et al. Automated tracking of the mitral valve annulus motion in apical echocardiographic images using multidimensional dynamic programming. Ultrasound Med Biol 2007;33:1389–99.
[11] Bland JM, Altman DG. Measuring agreement in method comparison studies. Stat Meth Med Res 1999;8:135–60.
[12] Jiang J, Hall TJ. A generalized speckle tracking algorithm for ultrasonic strain imaging using dynamic programming. Ultrasound Med Biol 2009;35:1863–79.
[13] Jiang J, Hall T. A parallelizable real-time motion tracking algorithm with applications to ultrasonic strain imaging. Phys Med Biol 2007;52:3773.
[14] Coats AJ. Ethical authorship and publishing. Int J Cardiol 2009;131:149–50.